MR DAMPER PERFORMANCE FOR SHOCK ISOLATION

Bogdan Sapiński
Maciej Rosół

Department of Process Control, AGH – University of Science and Technology
e-mail: deep@uci.agh.edu.pl; mr@ia.agh.edu.pl

The paper is focused on the shock isolation performance of a drivers seat whose suspension is completed with a linear magnetorheological fluid damper (MR damper). The aim of experimental investigations was to recognize the MR damper performance against shock effects. The experiments were performed on a linear damper of RD-1005-3 series manufactured by Lord Corporation operating in open loop and closed-loop system configurations under shock displacement-inputs (rounded pulses and square waves). In the first case, the MR damper was operating as a passive damper and in the second case, as a controllable damper for which real-time controllers were developed in the MATLAB/Simulink environment. The system performance for shock isolation was evaluated basing on measured system responses.

Key words: magnetorheological fluid damper, drivers seat, shock isolation, controller

1. Introduction

In recent years, MR fluid technology has spread rapidly and many MR devices and systems have been commercialized. In the automotive industry such products include: Delphi Automotives MagneRide^{TM} shock absorbers, Carreras MagneShock^{TM} automotive racing shocks and Motion Master Ride Management System (Carlson, 2003). These systems offer good performance for suppressing of unwanted vibrations using MR dampers. Experimental investigations reported in Choi *et al.* (2000), Sapiński (2003), Sapiński and Rosół (2003) confirmed the effectiveness of MR damper operation for vibro-isolation in a suspension system of a driver's seat support. An MR seat damper acts as an interface between the electronic control unit and the mechanical structure of the suspension. The damping characteristics of an MR damper can be varied continuously which allows full control of drivers seat vibrations with the use of

magnetic fields. Such a semi-active system uses external power only to adjust the damping and operates as a controller and set of sensors attached to the seat (Ahmadian, 1999). The controller determines the required damping force and automatically commands the damper to generate an appropriate force to reduce the amount of energy transmitted from the source of vibrations or shocks to the suspended equipment.

The aim of this paper is to evaluate the system performance for shock isolation through experimental investigation of shock isolation behaviour of a driver seat supported by the RD-1005-3 damper. For this purpose, the seat was tested under shock excitations (rounded pulses and square waves) in an experimental setup. It appears, however, that the seat vibrations are difficult to measure hence only their temporal effect could be quantified. Tests were run in open loop and closed-loop system configurations.

2.   Operating principle of MR damper

The MR seat damper employed in the tested seat suspension is a compact device fabricated by Lord Corporation. It was developed for drivers seats in vehicles (trucks, buses, agriculture tractors). The main benefits of the RD-1005-3 damper are: low voltage and current demands, precise and instantaneous control, continuously variable damping, simple electronics, real time control and long service life. A schematic diagram for the MR damper is shown in Fig. 1.
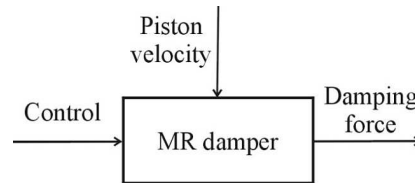
Fig. 1. Schematic diagram for MR damper

The inherent feature for the MR damper is high non-linear dynamic behaviour including hysteresis and step-like effects (Sapiński, 2002). This is due to special properties of the magnetorheological fluid (MRF) (Sapiński, 2004). The performance curves of velocity and control for the RD-1005-3 damper are provided in Fig. 2. It illustrates 3D-force-velocity-control curves captured in the range of applied current 0 to 0.2 A and piston velocity -0.4 to $+0.4$ m/s.

The MR damper is controlled using the pulse width modulation (PWM) method (Sapiński and Rosół, 2003). It is known that the RD-1005-3 response time is less than 25 ms (time to reach 90% of the maximal level during a 0 to 1 A
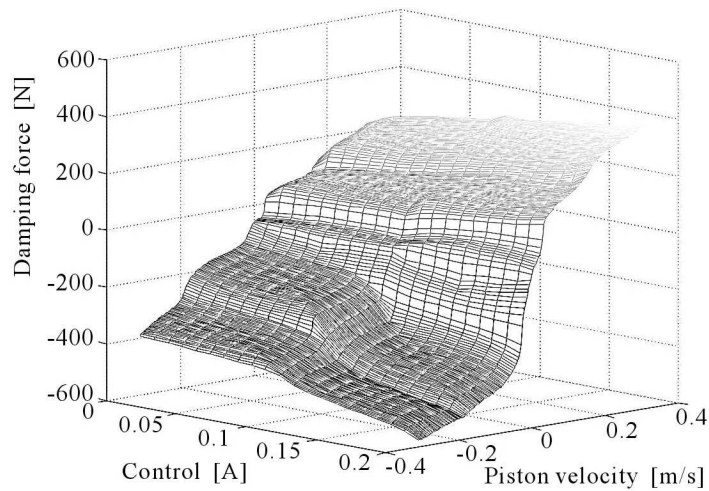
Fig. 2. Performance curves for RD-1005-3 damper

step input at velocity $51 \cdot 10^{-3}$ m/s, RD-1005-3 Product Bulletin, 2003). This time is dependent on an amplifier and power supply.

3. Shaping of excitation signals

In the experiments, displacement-input excitations were applied as rounded pulse shocks and square waves. The rounded pulse shock is analytically expressed by the formula

$$x_0(t) = X_0 \frac{\mathrm{e}^2}{4}(\gamma\omega_n t)\mathrm{e}^{-\gamma\omega_n t} \tag{3.1}$$

where γ is the parameter expressing the time of pulse duration in relation to the half-period of natural system vibrations. The parameter γ is given by the formula

$$\gamma = \frac{T}{2\tau} = \frac{\pi}{\omega_n\tau} \tag{3.2}$$

where
    τ –   duration of the square impulse with the area equal to that of the rounded pulse,
    ω_n –   pulsation of natural vibrations of the system,
    X_0 –   rounded pulse amplitude.

The chief advantage of the rounded pulse excitation is that its first and second derivatives assume limited values for all time instants t.

The frequency of natural vibrations of the seat obtained experimentally is 5 Hz (Sapiński, 2003). The desired amplitude of the rounded pulse was set to be $X_0 = 2.57 \cdot 10^{-3}$ m. After re-scaling associated with the signal passing through a C/A converter of the RT-DAC4 board and amplifiers of the control cubicle shaker, the maximum value of the rounded pulse equals $1.75 \cdot 10^{-3}$ m.
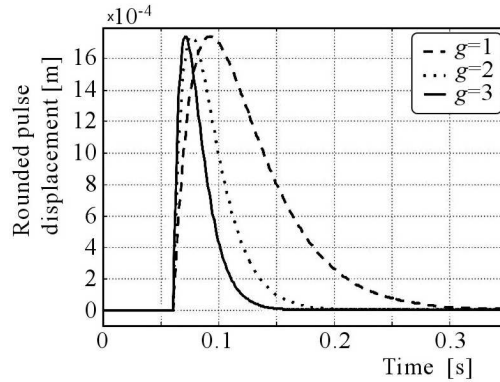
Fig. 3. Rounded pulse displacement for various values of γ

Time patterns of simulated rounded pulse displacements for various values of γ are provided in Fig. 3. Time patterns of simulated and measured rounded pulse displacements for $\gamma = 1$ and $\gamma = 3$ are compared in Fig. 4. It is readily seen that the rounded pulse signals are not perfectly transmitted by the shaker system. The distortions are apparent in the pulse patterns, particularly at high values of γ.
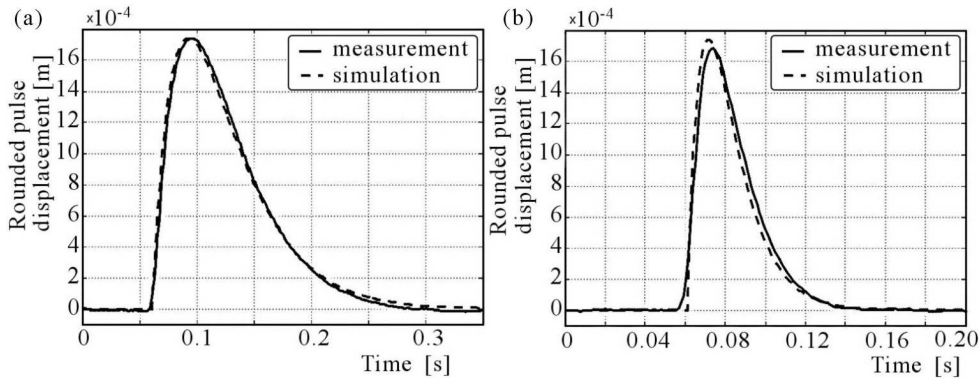
Fig. 4. Rounded pulse displacement: (a) $\gamma = 1$, (b) $\gamma = 3$

The square wave excitations were applied to find the properties of the system when shaker displacements underwent step changes. The square wave frequency was assumed to be 0.5 Hz which guarantees steady-state seat vibrations in between two subsequent wave edges.

4. Experimental setup

A schematic diagram of the experimental setup prepared for testing of the driver's seat against shock excitations is shown in Fig. 5.
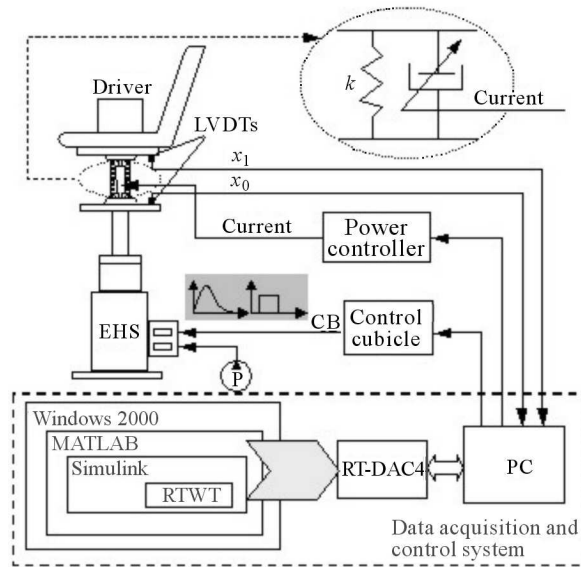
Fig. 5. Experimental setup – schematic diagram

The power supply circuit consists of an electro-hydraulic shaker (EHS) with a hydraulic pump (P) and a control cubicle (CB). Input-output data were acquired using a data acquisition and control system based on a PC (Pentium III/1GHz) with a multi I/O board (RT-DAC4), operating in the Windows 2000, MATLAB/Simulink and Real Time Windows Target (RTWT) environment. The shaker-base displacement x_0 and the frame displacement x_1 were measured with linear displacement transducers (LVDTs). The output signal from the controllers developed for the RD-1005-3 damper is the voltage in the range 0 to 5 V which, after leaving the power controller engineered by the authors is fed to the damper coil. Velocity and acceleration signals were reproduced by using derivative blocks. In Fig. 5, the RD-1005-3 damper is represented by an electrically controlled damping element parallel to the spring.

A general view of the drivers seat to be tested in the experimental setup is shown in Fig. 6.

A Simulink diagram developed for testing of the system is shown in Fig. 7. It enables us to: use the SA1 or SA2 controller, choose the type of displacement-input excitation for the shaker base (rounded pulse, square wave and others), measure and process signals of the shaker-base displacement and frame displacement.
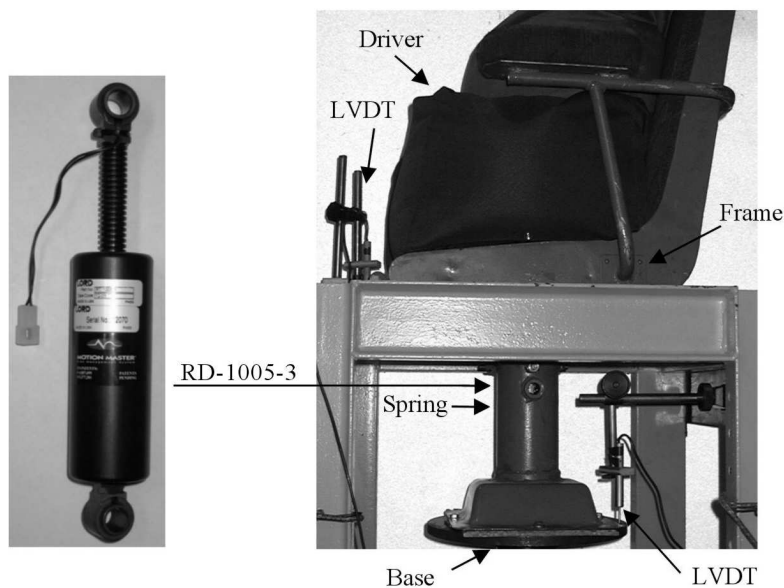
Fig. 6. Seat with RD-1005-3 ready for tests
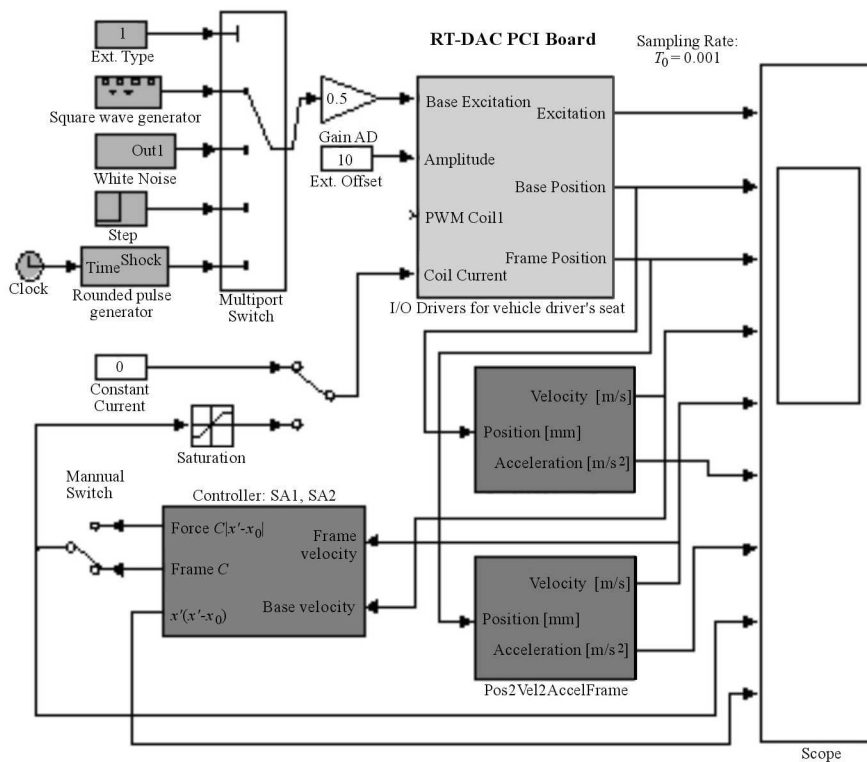
Fig. 7. Simulink diagram for shock isolation testing of driver's seat

The block unit designated as the "Rounded pulse generator" implements rounded pulse displacement–input excitations, in accordance with formula (3.1).

5.   Experiments

Experiments were conducted in open loop and closed-loop systems. The aim of open loop tests was to obtain the system response to various types of signals exciting the shaker base at various levels of current applied to the RD-1005-3 damper coil. The aim of closed-loop tests was to check the damping performance using the RD-1005-3 damper controlled by controllers developed specially for that purpose.

5.1.   Open loop system

Results obtained in the open loop system testing are shown as time patterns in Figs 8-13. Figure 8a provides seat responses for the current $I = 0\,\mathrm{A}$ and $\gamma = 1$, $\gamma = 2$, $\gamma = 3$. It appears that when the value of γ increases (i.e. the time of impulse duration gets shorter), the maximum value of the seat frame displacement will decrease. It follows from Fig. 9a that the higher the value of γ, the greater the maximum value of vibration acceleration. Moreover, the time required for the system to reach the steady state gets shorter.
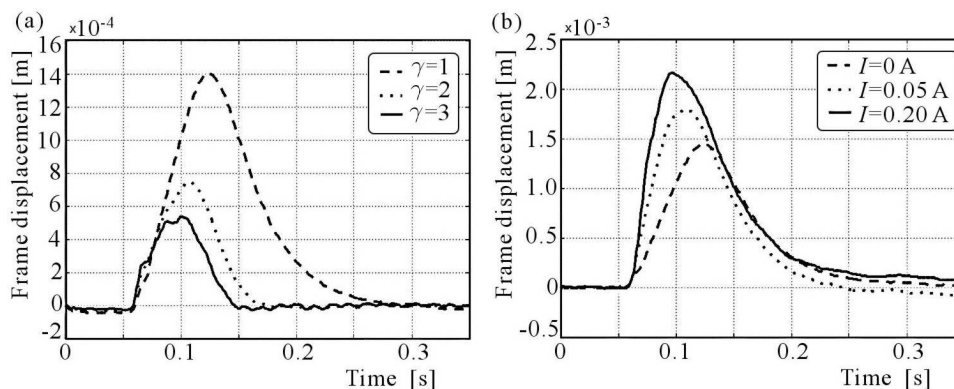
Fig. 8. Frame displacement in response to rounded pulses for: (a) $I = 0\,\mathrm{A}$ and various values of γ, (b) $\gamma = 1$ and various applied currents

The influence of the applied current level on the displacement and acceleration of the seat frame is shown in Fig. 8b and Fig. 9b. As the current level increases, the maximum values of the seat frame displacement and acce-

leration increase too. Throughout the investigated range of the applied current, there were no major changes in the time required to reach the steady state.
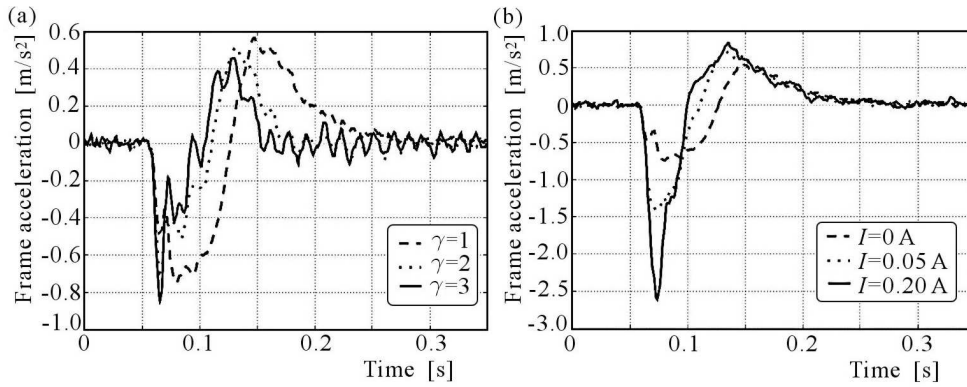
Fig. 9. Frame acceleration in response to rounded pulses for: (a) $I = 0\,\mathrm{A}$ and various values of γ, (b) $\gamma = 1$ and various applied currents

Figures 10a and 10b present the seat vibration acceleration obtained for square wave displacement-input excitations applied to the shaker base for $I = 0\,\mathrm{A}$ and $I = 0.10\,\mathrm{A}$. The base excitation signal (doted line) is scaled 500:1 and expressed in meters. Figs 10a and 10b provide sections of time patterns covering the period between the occurrence of ascending or descending wave edges and the instant the steady state is reached. As the current level increases, the amplitude of seat vibration acceleration rises too, and the time required to reach the steady state gets shorter. The variations of acceleration amplitude for various current levels are nonlinear.
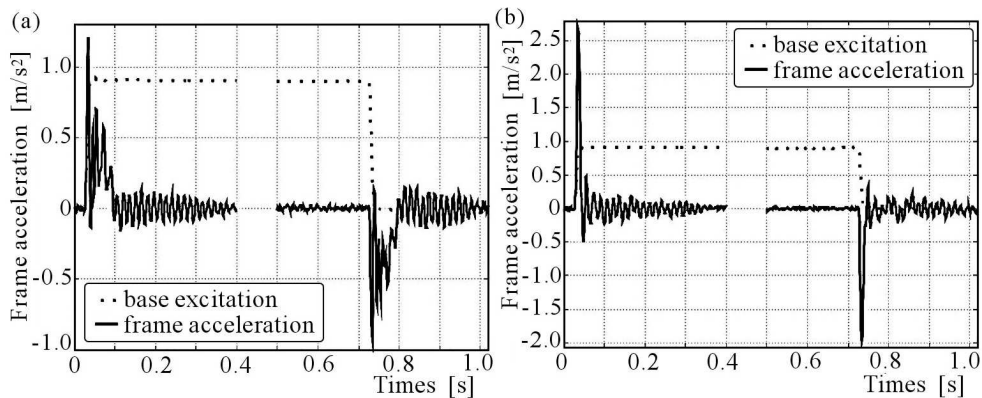
Fig. 10. Frame acceleration in response to square wave for: (a) $I = 0\,\mathrm{A}$, (b) $I = 0.10\,\mathrm{A}$

5.2. Closed-loop system

It is assumed that the operation of developed controllers for the RD-1005 damper, i.e. on-off controller (SA1) and continuous controller (SA2), is governed by equations (5.1) (Liu *et al.*, 2002)

$$\text{SA1}: \qquad I = \begin{cases} c_1 & \text{for} \quad \dot{x}_1(\dot{x}_1 - \dot{x}_0) \geqslant 0 \\ 0 & \text{for} \quad \dot{x}_1(\dot{x}_1 - \dot{x}_0) < 0 \end{cases}$$

$$\text{SA2}: \qquad I = \begin{cases} c_2|\dot{x}_1 - \dot{x}_0| & \text{for} \quad \dot{x}_1(\dot{x}_1 - \dot{x}_0) \geqslant 0 \\ 0 & \text{for} \quad \dot{x}_1(\dot{x}_1 - \dot{x}_0) < 0 \end{cases}$$

$$(5.1)$$

where
$\dot{x}_0$ – base velocity,
$\dot{x}_1$ – frame seat velocity,
$\dot{x}_1 - \dot{x}$ – relative velocity,
$c_1, c)2$ – constants.

The values of c_1 and c_2 depend on the maximum value of the applied current. The term $\dot{x}_1(\dot{x}_1 - \dot{x}_0)$ is called the velocity product. Time patterns of the seat vibration acceleration obtained in the closed-loop system completed with the controllers SA1 and SA2 and the time patterns in the open-loop system are compared in Figs 11a and 11b. In both cases, the rounded-pulse displacement input excitations were applied. It is readily seen that the controllers SA1 and SA2 do not provide any reduction to the seat vibration acceleration while compared to the open loop system.
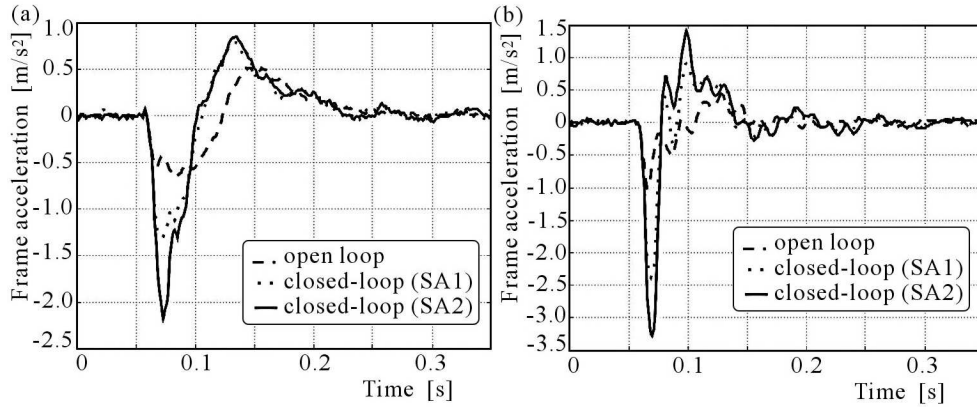
Fig. 11. Frame acceleration in response to rounded pulse for: (a) $\gamma = 1$, (b) $\gamma = 3$

The experiments when square wave excitations were applied to the shaker base allow similar conclusions to be drawn as in the case of rounded pulse

excitations. That was confirmed by the time patterns of seat vibration acceleration obtained for the closed–loop system with the controllers SA1 and SA2 (Fig. 12).
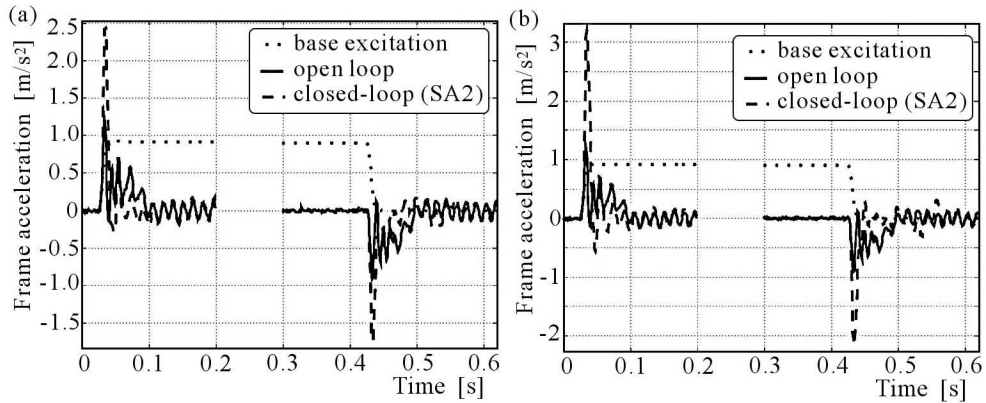
Fig. 12. Frame acceleration in response to square wave for closed-loop system with: (a) SA1, (b) SA2

A comparison between the performance of the open loop and closed-loop systems (with the controllers SA1 and SA2) is shown in Fig. 13.
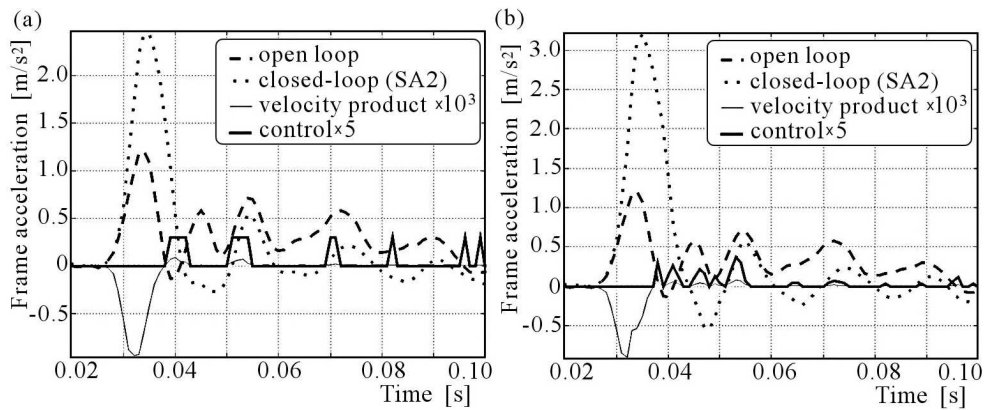
Fig. 13. Closed-loop system with: (a) SA1, (b) SA2

It is seen that the control signals for the controllers SA1 and SA2 are generated in accordance with formulas (5.1). Nonzero values of the control signal (i.e. current in the MR damper coil) occur only when the term of velocity product is positive. It is reasonable to expect, therefore, that at the zero current, the time patterns of seat acceleration obtained for the open loop and closed-loop system configurations and for the same initial conditions ought to

be similar. Actually, the acceleration of seat vibrations is much greater in the closed-loop system, which is best seen in Fig. 13a (time from 0.026 to 0.038 s) and in Fig. 13b (time from 0.026 to 0.037 s).

6.   Conclusion

The paper summarises results of an experimental programme where a drivers seat equipped with an MR damper was subjected to shock displacement excitations. Responses of open-loop and closed-loop systems (with the controllers SA1 and SA2) are compared, leading us to the conclusion that the action of these two controllers fails to reduce the vibration acceleration in the system. The reasons for this state of affairs are attributable to the properties and operating principles of the electromagnetic circuit of the RD-1005-3 damper. This problem is illustrated graphically in Figs 14a and 14b, showing the current levels and damping force under triangle displacement-input excitations of the base and PWM voltage signal across coil clamps.

Figure 14a shows base excitations (frequency 1 Hz, amplitude $10 \cdot 10^{-3}$ m) and PMW excitations (frequency 4 Hz, amplitude 0.8 V, width factor 0.2/0.8). It is apparent (Fig. 14b) that the time required for the current and damping force to stabilise is still considerable. The times t_I and t_F are understood as times required to reach 95% of the steady value in conditions of step variations of voltage across the coil clamps. The measurement results reveal that the times required for stabilisation of the current in the coil and the damping force are:

- for the ascending edge of the voltage signal:

  $t_I = 65 \cdot 10^{-3}$ s, $t_F = 150 \cdot 10^{-3}$ s,

- for the descending edge of the voltage signal:

  $t_I = 101 \cdot 10^{-3}$ s, $t_F = 78 \cdot 10^{-3}$ s.

Figure 14b shows base excitations (frequency 4 Hz, amplitude $1.5 \cdot 10^{-3}$ m) and PWM excitations (frequency 20 Hz, amplitude 0.8 V, width factor 0.2/0.8). It appears that as the frequency of the PWM control signal increases, neither the current in the coil nor the damping force will reach the steady value.

In the case considered in this study, the current level would vary from 0 to 0.2 A. One has to bear in mind that the times required to stabilise the current and the damping force chiefly depend on the parameters of the power controller and on the current level in the coil. The measurement results obtained for the current varied from 0 to 1.0 A reveal that the times required for stabilisation of the relevant parameters changed significantly, and now are equal to:
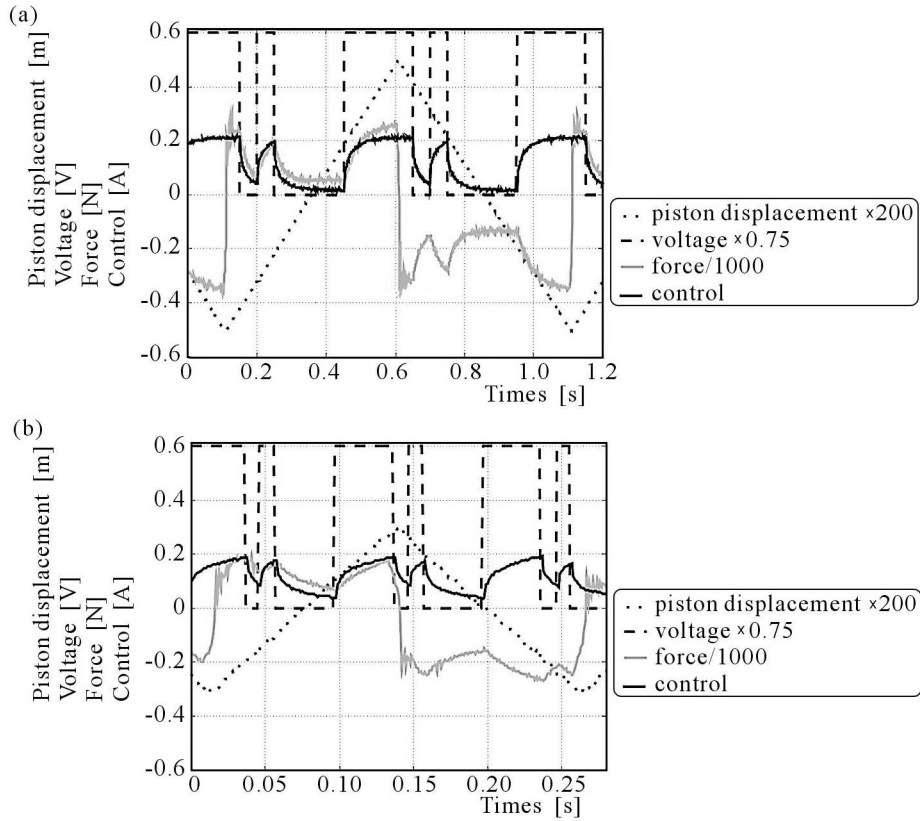
Fig. 14. Force and current responses in RD-1005-3 damper: (a) PWM frequency 4 Hz, triangle displacement-input 1 Hz, (b) PWM frequency 20 Hz, triangle displacement-input 4 Hz

- for the ascending edge of the voltage signal:

$t_I = 48 \cdot 10^{-3}$ s, $t_F = 56 \cdot 10^{-3}$ s,

- for the descending edge of the voltage signal:

$t_I = 148 \cdot 10^{-3}$ s, $t_F = 173 \cdot 10^{-3}$ s.

This is a consequence of the magnetic circuit reaching the state of saturation.

Concluding remarks why the system time of response to changes of the control signal is prolonged might be as follows: nonzero time of the MR damper force stabilisation, magnetic residues in the MR damper components, delays due to current signal stabilisation at the output of the power controller.

References

1. AHMADIAN M., 1999, On the isolation properties of semi-active dampers, *Journal of Vibration and Control*, **217-232**

2. CARLSON J.D., 2003, Engineering with magnetorheological fluids, *Proc. of Smart03 Workshop*, Warsaw, to be published

3. CHOI S.B., LEE B.K., NAM M.H., CHEONG C.C., 2000, Vibration control of a MR seat damper for commercial vehicle, *Smart Structures and Integrated Systems*, N. Werely (Edit.), *Proc. of SPIE*, **3985**

4. LIU Y., MACE B., WATERS T., 2002, Semi-active dampers for shock and vibration isolation: algorithms and performance, *Proceedings of International Symposium on Active Control of Sound and Vibration*, UK, 1121-1132

5. Lord Corporation: RD-1005-3 Product Bulletin, 2003

6. SAPIŃSKI B., 2002, Parametric identification of MR linear automotive size damper, *Journal of Theoretical and Applied Mechanics*, **40**, 703-722

7. SAPIŃSKI B., 2003, Autonomous control system with fuzzy capabilities for MR seat damper, *Archives of Control Sciences*, **13** (XLIX), 2, 115-136

8. SAPIŃSKI B., 2004, *Linear Magnetorheological Fluid Dampers for Vibration Mitigation: Modelling Control and Experimental Testing*, Monography 128, Cracow (to be published)

9. SAPIŃSKI B., ROSÓŁ M., 2003, Real-time controllers for MR seat damper, *Proc. of Smart03 Workshop*, Warsaw (to be published)

Efektywność zastosowania tłumika magnetoreologicznego w izolowaniu obciążeń udarowych

Streszczenie

W artykule rozważono problem wibroizolacji zawieszenia fotela kierowcy z liniowym tłumikiem magnetoreologicznym (MR). Celem badań była ocena efektywności działania tłumika MR w układzie zawieszenia fotela poddanego działaniu wymuszeń impulsowych. Eksperymenty przeprowadzono dla układu z otwartą i zamkniętą pętlą sprzężenia zwrotnego. W badaniach wykorzystano tłumik MR (model RD-1005-3) firmy Lord Corporation. Fotel poddawano wymuszeniom kinematycznym typu prostokątnego i symulującego wstrząsy. Zaprojektowane regulatory zaimplementowano w programie MATLAB/Simulink, a następnie uruchomiono w środowisku czasu rzeczywistego oferowanego dla systemu operacyjnego Windows 2000/XP przez przyborniki RTW/RTWT. Oceny efektywności układu wibroizolacji fotela z tłumikiem MR dokonano na podstawie pomiarów odpowiedzi dynamicznych zawieszenia.